THREE DIMENSIONAL BOUNDARY LAYER ON A ROTATING CYLINDER

WILLIAM H. BOWLING
AND
JAMES G. HAYES

THREE DIMENSIONAL BOUNDARY LAYER

ON A ROTATING CYLINDER

by

LT. WILLIAM H. BOWLING, U.S. NAVY

B.S., U.S. NAVAL ACADEMY (1951)
B.S.(A.E.), U.S. NAVAL POSTGRADUATE SCHOOL (1958)

and

LT. JAMES G. HAYES, U.S. NAVY

B.S.(Math.), BALDWIN-WALLACE COLLEGE (1951)
B.S.(A.E.), U.S. NAVAL POSTGRADUATE SCHOOL (1958)

SUBMITTED IN PARTIAL FULFILLMENT OF THE
REQUIREMENTS FOR THE DEGREE
OF MASTER OF SCIENCE IN
AERONAUTICAL ENGINEERING

at the

MASSACHUSETTS INSTITUTE OF TECHNOLOGY

JUNE, 1959

THREE DIMENSIONAL BOUNDARY LAYER ON A ROTATING CYLINDER

by

William H. Bowling
and
James G. Hayes

Submitted to the Department of Aeronautics and Astronautics on May 25, 1959, in partial fulfillment of the requirements for the degree of Master of Science in Aeronautical Engineering.

ABSTRACT

The normal boundary layer found in rotating machinery is skewed and has a three dimensional velocity profile. Better understanding of skewed boundary layers should lead to improved turbo-machinery design. This study was undertaken to investigate skewing of the boundary layer on the outside surface of a rotating cylinder. The cylirder was rotated at different speeds to give values of the parameter Ω=(pipe surface velocity/air axial velocity) varying from zero to two. The effect of Reynolds' Number was investigated by varying the air axial velocity from 25 to 75 feet per second while holding Ω constant.

The technique of pressure measuring and visual observation of carbon black patterns was used in this investigation to determine the effects of the rotating cylinder on the boundary layer. It was found that the skewed boundary layer was quasi-collateral in nature with a collateral sub-layer. The axial and tangential displacement thicknesses increased with Ω although negligible change was noted in the actual boundary layer thickness. The tangential component of velocity increased with distance along the axis, resulting in a decrease in static pressure due to centrifuging. This phenomenon induces a favorable pressure gradient in the axial direction; however, the change in velocity due to this static pressure change is small. The problem of measuring angle of flow in a skewed boundary layer with steep velocity gradients was encountered. Evidence indicated the angular measurements were low, and that the flow was turned more than indicated by the yaw probe measurements.

Thesis Supervisor: Edward S. Taylor
Title: Professor of Aircraft Engines

ACKNOWLEDGEMENTS

The authors wish to express their gratitude to all those immediately concerned with this thesis and to the many encouraging friends at the M.I.T. Gas Turbine Laboratory. Special acknowledgement goes to Prof. E.S. Taylor, thesis advisor, for his guidance and suggestions throughout the course of endeavor. Thanks of appreciation are given to Mr. Baugh and his staff who provided the many odds and ends required. The machine work personally done by Mr. Gugger and by his staff should receive mention as well as the many helpful suggestions contributed by Prof. Y. Senoo and Mr. R. Schwind.

Typing credit is given to Miss Joan McRill.

TABLE OF CONTENTS

TITLE PAGE

ABSTRACT

ACKNOWLEDGEMENTS

TABLE OF CONTENTS

SYMBOLS

1. INTRODUCTION 1

2. DESCRIPTION OF APPARATUS 3

2.1 The Wind Tunnel 3

2.2 Intake Nozzle 3

2.3 Test Section 4

2.4 Diffuser and Fan 6

3. PROBES AND INSTRUMENTATION 7

3.1 Probes 7

3.2 Pressure Sensing Apparatus 8

3.3 RPM Measurements 9

4. EXPERIMENTAL PROCEDURES 9

4.1 Static Pressure 9

4.2 Reference Dynamic Head 10

4.3 Rotation Effect Study 10

4.4 Reynolds' Number Effect 12

4.5 Angular Measurements 12

4.6 Carbon Black Traces 13

5. RESULTS AND DISCUSSION 13

6. SUMMARY AND CONCLUSIONS 17

REFERENCES AND BIBLIOGRAPHY 19

FIGURES

APPENDICES

SYMBOLS

P_o Total Pressure

P_s Static Pressure

q Dynamic Pressure

R_e Reynolds' Number

S Cylinder Surface Velocity

u Axial Velocity in the Boundary Layer (Fixed Coordinates)

U Free Stream Velocity (Common to Fixed and Rotating Coordinates)

v Resultant Velocity in the Boundary Layer (Fixed Coordinates)

w Transverse Velocity in the Boundary Layer (Fixed Coordinates)

x Distance in the Longitudinal Direction

y Distance Normal From the Cylinder Surface to Probe ℄.

δ^* Displacement Thickness

$\frac{\delta^*_{ar}}{\delta^*_a}$ Thickening Factor (Ratio of Axial Displacement Thickness Without Rotation to that With Rotation)

ρ Density

η Transverse Velocity Relative to the Cylinder

Ω Ratio of Cylinder Surface Velocity to Axial Velocity of the Free Stream

THREE DIMENSIONAL BOUNDARY LAYER ON A ROTATING CYLINDER

1. INTRODUCTION

A better understanding of the three-dimensional boundary layer as it applies to turbo-machinery has been emphasized in recent research work conducted at the Gas Turbine Laboratory at M.I.T. Only with a study and understanding of the mechanics of the true nature of the flow, can the performance of turbo-machinery be improved. In the past, analysis of flow has been based on simplification to two dimensional and laminar flows which are actually limited in applicability.

The three dimensional or skewed boundary layer is generated by two basic methods in turbo-machinery. The turning of the boundary layer from the main flow is one. The flow becomes skewed due to the action of the transverse pressure gradient. This type of flow is commonly called " secondary flow" and can occur along the end wall of a compressor cascade blade passage.

The second method of skewing the flow is by the action of shear forces alone, such as would develop in the boundary layer of axial flow on a rotating cylinder. In compressors and turbines, this phenomenon occurs where a casing encounters a rotating hub.

An experimental investigation has been undertaken to determine the nature of the skewing by the latter method. This work is similar to an earlier Gas Turbine project

conducted by A.H. Stenning [1] *. In his work Stenning generated a skewed boundary layer on the inside of a rotating pipe. His experiment was of a preliminary nature but the following results were indicated:

(1) As the rotation of the pipe increased, the axial velocity profile flattened.

(2) At a critical surface to axial velocity ratio (Ω), depending on the length of the pipe, the velocity profile remained unchanged.

Stenning was limited in pressure measurements by the configuration of his apparatus. This deficiency was overcome in the present experimental work through the use of a test section where the pressure measurements were obtained on the outside of a rotating cylinder.

The skewed boundary layer has recently been discussed in detail by E.S.Taylor [2] . The skewed boundary layers found in practice have been noted to be a combination of a regular two dimensional (collateral) part and a part that would be collateral if viewed from a moving reference frame. The latter type is called quasi-collateral. In practice, skewed boundary layers have been found to be quasi-collateral with a collateral sub-layer on the surface. Boundary layers of this type experienced by several authors are presented in a report by Johnston [3] .

- -

* Numbers in brackets refer to references listed at the end of the thesis.

2. DESCRIPTION OF THE APPARATUS

2.1 The Wind Tunnel.

A small, low speed, open wind tunnel was designed and built under the requirements of the problem being investigated. Non-rotational, turbulent, parallel, axial flow was provided over the surface of a long cylinder. A portion of this cylinder could be rotated about its longitudinal axis at a constant peripheral velocity. Accomodations for pressure measurements were installed in the vicinity of the rotating cylinder. Control features of the tunnel permitted axial flow and cylinder peripheral velocities of any desired combination.

The tunnel consisted of three major components: the intake nozzle; the test section and the rotating cylinder (including the drive apparatus); and the diffuser and exhaust fan, as shown in Figs. 1 and 2.

2.2 Intake Nozzle.

The intake nozzle received air radially and delivered it to the test section in an axial direction. This particular arrangement accommodated a relatively short drive shaft linkage between the rotating cylinder and the drive mechanism. In designing the nozzle, several criteria were kept in mind. First, the velocity in the free stream had to be a constant in the radial direction. Secondly, it was desired to have the ratio of the inlet area to the outlet area equal to two. This would reduce losses in total pressure when a screen was installed around the inlet area

since the velocity at the inlet would be low. Losses in total pressure are directly proportional to the dynamic head and thus the square of the velocity. Thirdly, no place along the surface should the velocity decrease to less than 60 percent of its maximum value. The latter requirement would forestall flow separation along the walls.

For design purposes, the cross section profile of the intake was assumed to be that of the flow pattern of a liquid jet deflected by a perpendicular boundary, [Ref. 4] . By the use of an electrical analog of Teledeltos paper cut to the shape of the proposed intake profile, the potential flow was determined, and by the method of Appendix A, the velocity profile was computed for a three dimensional nozzle. Alterations on the profile were made by a trial and error method until the desired design criteria were fulfilled. The final profile selected from Teledeltos paper is shown in Fig.3. A velocity profile survey of the tunnel test section after construction indicated that the design method was adequate. The U.S.Naval Shipyard, Boston, constructed the two piece wooden intake which was then finished by painting and waxing.

2.3 Test Section.

The test section consisted of an outer cylindrical cylinder of 14 inch I.D. steel pipe 22 inches in length. A six inch O.D. aluminum pipe was mounted through the center of the test section along the longitudinal axis and was faired into the intake at one end and the diffuser at the other end. A 10 inch section of this inner aluminum pipe

was designed to rotate concentrically within $\pm$ 0.001 inch.

Provision for mounting a traversing probe mechanism at ten probing stations along the axis of the test stations was installed on the outer pipe as well as a flush, plastic, 4 x 10 inch window to permit observation of the traversing operation. Fig. 2 illustrates the relative positions of the probing stations to the rotating cylinder. Forty-one static pressure taps of 0.031 inch I.D., four equally spaced for each probing station, were carefully placed in the wall of the test section. Care was taken to deburr and to smooth the static taps. One static tap was installed on the inner pipe immediately aft of the intake, three inches upstream of the rotating cylinder leading edge.

Solid aluminum flanges supported the rotating cylinder on a steel drive shaft. Initially, the drive consisted of modified, spoked, cast iron pulley wheels and a hollow drive shaft. Unacceptable vibrations resulted from this first arrangement, necessitating redesign. The drive shaft, which extended from one end of the rotating cylinder through the intake nozzle, was mounted on three ball bearings; two sealed SKF type at each end, and one SKF self aligning type positioned at the front end of the rotating cylinder. Provisions for grease retaining and cylinder positioning were built into the self aligning bearing mount. The spacing between the fixed and the rotating section was set at 0.018 inches. Rotation speeds of 4000 RPM were maintained for 45 minutes without serious overheating using grease lubrication.

The drive assembly design included a short pulley belt linkage to a Speed Ranger 1/2 H.P. motor with variable drive capable of a 1 to 16 speed ratio. An early arrangement utilizing a Toledo pulley was considered unsatisfactory due to vibrations at several critical speeds, apparently the result of belt deflections.

2.4 Diffuser and Fan

The diffuser consisted of an outer cone mating the test section flange with the fan casing flange and a concentric inner cone extending from the six inch aluminum pipe to the hub of the fan blades. A survey of the literature showed appropriate diffuser design data for this geometry (three dimensional) was unavailable. The design criteria finally decided upon was a total diverging angle between the two surfaces of the inner and outer cones of 4.45 degrees. This was based on considerations of area/length ratios and maximum allowable diffusion angles reported for two dimensional flows.

The exhaust fan was a single stage axial machine having a rating of 6000 cfm at two inches of water pressure rise. The fan casing diameter was 25 1/8 inches. Two speeds of fan rotation were available, 1765 and 1175 RPM. Free stream velocity in the test section was controlled by bleeding air at a circumferential slot between the diffuser and fan casing. The fan was mounted on coasters in a channel track; therefore, the fan motor could be positioned manually in relation to the rest of the apparatus

which was bolted to the floor.

3. PROBES AND INSTRUMENTATION

3.1 Probes

The probes used are shown in Fig. 4 with the exception of a larger total pressure probe installed in the intake which was used as a reference. The two working probes were of the three hole cobra configuration consisting of a total head tube in the center flanked by two yaw tubes whose tips were ground off to an angle of 60 degrees for maximum yaw sensitivity. The dimensions of the probes were determined by measurements on a microscope and were as follows:

	A	B
Pitot tube I.D:	0.016 in.	0.008 in.
Center line to bottom:	0.011 in.	0.005 in.

The use of probe A was discontinued when it was found to be too large to measure pressure very close to the cylinder surface. Because of the nature of the pressure sensing equipment, no difficulty was encountered in response rates when switching to the smaller probe B. The added restriction of a rotating surface required a clearance of 0.003 inch from the surface to the bottom of the probe to prevent contact from the surface deflection and diameter increases at high rotation speeds. The latter was calculated to be about 0.0005 inch. The clearance from the probe bottom to the surface was measured by a feeler gauge.

The cobra probes were mounted on a traversing device as

shown in Fig. 5. The probe relative to the cylinder is shown in Fig. 6. Installed on the traversing head was a protractor on which angles could be measured from a pointer secured to the probe stem. The traversing head which moved the probe and protractor perpendicular to a tangent on the surface of the cylinder was driven by a screw arrangement which translated 0.1 inches per revolution. A dial mounted on the screw was marked in increments of 0.001 inches. The entire traversing device was secured in place at each station by two screws. Contact surfaces were all machined to insure accuracy.

Plastic plugs which fitted flush to the inner wall sealed off stations not being probed.

3.2 Pressure Sensing Apparatus

Differentials between total and static pressures, and between static and atmospheric pressures were sensed by Dynisco strain gauge pressure transducers. The bridge circuit containing the transducers was balanced by a calibrated potentiometer circuit which in turn was a measure of pressure. The system was calibrated by a micromanometer and found to be linear over the entire allowable pressure range with error of less than 1 percent. Dynamic Instrument Company, Cambridge, Massachusetts, was the supplier of the equipment.

The nulling of the pressure differences of the yaw tube for measuring angles was accomplished on a galvanometer with a Statham strain gauge pressure transducer manufactured by Statham Laboratories, Los Angeles, California.

A reference total pressure probe in the intake was provided to be used with a reference static pressure tap, and both were connected to a Meriam Instrument Company, Type G.P.-6 inclined manometer using Meriam red oil (sp.gr:0.827). The manometer calibration display was in inches of water.

3.3 RPM Measurements

Since the surface velocity of the rotating cylinder was linear with RPM, an accurate measurement of drive shaft revolutions was required. Initial setting on the reduction gearing was accomplished with a strobotac. A fine setting was then made with a HASLER Speed Indicator placed on the drive shaft. After the oil temperature had reached its operating range, the drive motor was capable of maintaining the RPM within 0.2 percent for a period of 15 minutes.

4. EXPERIMENTAL PROCEDURE

4.1 Static Pressure

Measurements were made at all the static pressure taps with the cylinder stationary. A curve was faired through the plot of these pressures with axial distance. The static tap at each station that read most nearly the mean was then chosen as the static pressure source for that particular station.

The pressure difference between static and atmospheric was read on the Dynisco Instrument from a pressure transducer. A manifold arrangement permitted choice of static pressure. The barometer was recorded regularly, permitting the static pressure to be computed.

Measurements were made of the radial static pressure

distribution by use of three different pressure probes: two pitot-static type L-shaped probes, and a disc-static probe. No change in pressure with rotation was noted.

Measurements were also made of all static pressure taps with the cylinder rotating at maximum peripheral speed of 100 feet per second, and with free stream velocities from 25 to 100 feet per second. No change was noted in the static pressure with rotation.

4.2 Reference Dynamic Head

The total pressure from the permanent total head tube in the intake nozzle was lead to one side of an inclined manometer. Static pressure from an arbitrarily selected static pressure tap was introduced to the other side of the inclined manometer. The difference of these pressures, in inches of water, served as a reference dynamic head. The reading was noted continually throughout the operation before each data reading to assure that there was no change in the flow.

4.3. Rotation Effect Study

Pressure measurements through the boundary layer were made at each station starting at the surface of the cylinder and traversing radially outward. Clearance of 0.003 inch between the probe and the surface was measured by a feeler gauge. The control space between the blower and the diffuser was adjusted to give a constant free stream velocity. Total pressure from the traversing cobra probe was led to one side of a pressure transducer, and the particular static pressure

for that same station was led to the other side. The difference was measured on the Dynisco Indicator. The yaw tubes of the cobra were nulled on a galvanometer and the angular indications read from the protractor.

To keep within the limits of the pressure transducers, and to permit lower RPM, the initial runs were made with the free stream velocity held constant at 67 feet per second at station number two instead of the design velocity of 100 feet per second. Observations were taken 1/2 inch upstream, and 1/2, 3 1/2, 6 1/2, and 8 1/2 inches downstream of the leading edge of the rotating cylinder. The resulting changes in the axial velocity profiles are shown in Fig. 7. However, polar plots of these tests coupled with the information obtained from the Reynolds' Number Effect tests, as described in the next section, showed that more information was desireable about the boundary layer nearer the cylinder. Consequently, a new probe was obtained to give readings closer to the cylinder surface, sandpaper was added upstream of the rotating section, a lower velocity of 50 feet per second was selected for the free stream velocity, and runs at $\Omega = 2$ were made also.

For a variation to the procedure, the free stream was adjusted to give 50 feet per second at each station instead of at station two. This was done to give a more exact value of Ω at each station while maintaining a constant RPM setting for all stations. The resulting changes in transverse velocity profiles are compositely shown in Fig. 8. The individual station velocity profiles are shown in Figs. 9,10,11, and 12.

Polar plots of the axial and transverse velocities at the different values of Ω are shown in Figs. 13,14, and 15.

4.4 Reynolds' Number Effect

A range of three to one in Reynolds' Number was obtained by varying the free stream velocity from 25 to 75 feet per second. A value of Ω = 1.0 was maintained for all runs. Station number six was used for this test as it was well downstream from the leading edge of the cylinder and skewing was well developed.

Velocities of 25, 50, 67, and 75 feet per second were utilized. The required RPM for Ω = 1.0 were then 960, 1915, 2570, and 2875 respectively. The axial and transverse velocity profiles obtained are presented in Fig. 16, and a polar plot of velocities is presented in Fig. 17.

4.5 Angular Measurements

The flow direction of the boundary layer was measured by moving the cobra probe until the two side yaw tubes indicated a null reading on the galvanometer. The measurements of angle with 50 feet per second free stream flow and no cylinder rotation showed there to be no skewing of the flow and showed it to be axially directed. Consequently, all angular measurements of the skewed flow were related to the free stream angle. However, plotting of the data indicated the angular measurements were not as expected near the wall. Further measurements of the flow angle were made by maximizing readings of the total pressure tube as discussed in Section 5. Angles on the surface were also measured from carbon traces

as discussed in Section 4.6. Appendix C explains the angles and velocity vectors.

4.6 Carbon Black Traces

Fig. 18 shows the traces on the surface of the cylinder made by painting on a suspension of finely divided carbon black in kerosene. The traces were made for a free stream velocity of 50 feet per second and values of Ω = 0.3, 1.0, 1.5, and 2.0. The directions of the limiting streamlines were measured at each station by aligning a protractor with the test section and sighting along the carbon trace. The angles measured agreed in general within $\pm$ 2 degrees of the expected angle indicated by the polar plots of velocity. The angle measured is shown in Appendix C.

5. Results and Discussion

Rotation of the cylinder distorted the velocity profiles, resulting in the displacement thickness increasing with increased Ω. The thickening factor of $\delta^*_{ar}/\delta^*_{a}$, plotted in Fig. 19, increased with distance downstream and appeared to reach a limiting value at Ω = 1.0 for the case where the free stream velocity was maintained constant at station two. However, for the case where the free stream velocity was maintained constant from station to station, a limiting value was not reached, although the thickening factor did increase with distance downstream. The former is in agreement with the work of Stenning [1]. He formulated a length-diameter ratio correlation with the value of Ω for limiting the thickening factor. For the latter case of no limit it is quite

possible that increasing Ω above two, a limiting value could be achieved. Furthermore, the adjustment of the velocity precludes normal boundary layer growth and thus the two methods cannot be quantitatively compared. Appendix C contains a description of the polar plots. Polar plots of the velocity in Figs. 13, 14, and 15 indicate that the nature of the skewed flow is of two quasi-collateral sections. The sub-layer, as viewed from the rotating cylinder coordinates, was collateral. Thus, relative to the rotating cylinder, this is the usual type of skewed boundary layer as discussed by Taylor [2] . The polar plots agreed in nature with those of several authors presented in a report by Johnston [3] . The lamp-black traces corroborated the limiting streamline direction as shown on the polar plots. Velocities near the cylinder surface plotted somewhat off the curve. This is explained by an error introduced into the yaw probe indication in the skewed boundary layer with the skewed steep velocity gradients near the cylinder surface. Appendix B contains a discussion of this phenomenon. The angles measured by maximizing readings of the total pressure of the center hole of the three-hole cobra probe indicated original angle readings were as much as seven degrees in error. This would make the points fall off the curve. Correction for this angle error is indicated on the curves of Figs. 13 through 15. The angles measured by the total pressure method were corroborated by the carbon black traces. This problem points up one of the basic difficulties in three-dimensional boundary layer study. Yaw measurement

in velocity gradients has been treated by Lima [5] , indicating that much remains to be accomplished.

It can be seen from Fig. 8 that for the same radial distance, the transverse velocity component is greater downstream, but the velocity gradient is less. This effect is noted from the leading edge aft, and the flow upstream of the leading edge is unaffected by the cylinder rotation. The travel of the shear wave upstream is much less than the velocity moving the air downstream.

The polar plot of Reynolds' Number Effect, Fig. 17, indicates that the angle between the axial center line and the collateral sub-layer was unaffected. Within the R_e range observed, then, the limiting streamlines were unaffected, and the remainder of the skewed boundary layer was somewhat altered. The axial velocity profiles were similar for both $\Omega = 0$, and $\Omega = 1.0$; however, there was an indication of laminar flow for the 25 feet per second runs. The transverse velocity components were larger at the lower R_e for the same radial location, although, the shapes of the profiles were similar.

Investigations with a hot-wire anemometer indicated no regular interruptions of the random turbulence as would occur with vortices being formed. There was an apparent stability increase with higher Ω as evidenced by decreased amplitudes and increased frequencies on the oscilloscope. The latter would be expected from the favorable pressure gradient generated by the centrifuging of the cylinder.

The increase of transverse velocity with axial distance results in a decrease in static pressure along the cylinder. The favorable pressure gradient here is opposite to that in the work of Stenning, where he was measuring the boundary layer on the inside of a cylinder. The velocities were computed using the static pressure at the outer wall of the test section. Thus the velocities computed would be too low, since assuming $P_o - P_s = 1/2\ \rho\ v^2$ means that if the actual static pressure is less, the velocity will be greater.

Graphical integration of the change in static pressure gave results that are plotted in Fig. 17. Until station eight is reached, the drop in static pressure with distance due to centrifuging is greater than the initial static drop in the pipe. However, the change in pressure along the pipe is seen from Fig. 20 to be no more than about two percent of the total head, so the velocities will not be affected greatly. The main effect of the centrifuging is the resulting pressure gradient along the pipe. The change was almost linear with distance along the pipe. A change of 0.067 psf was observed over a distance of 9 1/2 inches from the leading edge of the cylinder to station eight. In Fig. 20 the effect of the centrifuging is compared to the static drop existing without rotation, and a third curve of the sum of the two effects was graphically computed and plotted.

Several suggestions for the continuation of the work can be offered. Chief among these is the solution of the problem

of getting measurements further into the boundary layer. Efforts along this line were rewarding, but it would be better to more accurately define the flow direction near the surface. Also, confirmation of the limiting streamlines by carbon black traces would be desireable for the R_e effect tests. The end of the cylinder where the skewed boundary layer passes onto the non-rotating part should be investigated. It is felt that some difficulty might be encountered in doing this since the static pressure change with distance along the pipe is most pronounced toward the rearward area. A modification to measure the static pressure on the rotating surface would be desireable. Finally, the challenge of angular measurement ought to be met, for concrete conclusions as to correct flow direction is basic to an understanding of the three dimensional boundary layer.

6. SUMMARY AND CONCLUSIONS

Investigation of the effect of a moving surface on the boundary layer created by through flow has been studied by rotating a cylinder and flowing air axially along its longitudinal axis. Distortion of the boundary layer takes place, and the displacement thickness of the axial component of velocity is thickened. The factor of thickening is greater downstream and at higher values of Ω, the ratio of the cylinder surface velocity to the free stream through flow velocity. The transverse velocity components' main effect is to cause a pressure gradient along the pipe. This centrifuging action induces a favorable pressure gradient as the

boundary layer is on the outer surface of the cylinder. The effect of the pressure change on the computed velocity is negligible.

Measurement of flow angles by yaw pressure probes of the cobra variety is considered to be somewhat unreliable in the flow regime near the rotating surface. The skewing of the flow and the steep velocity gradient cause blocking by the center total head probe. This results in an angular indication that is less than the actual flow deviation.

A turbulent quasi-collateral boundary layer with a collateral sub-layer was observed. This supports the supposition that the majority of skewed boundary layers are of this type. Limiting streamlines were measured by carbon black traces and corroborated the hypothesis that yaw probe angle measurements were erroneous. Variation of Reynolds' Number showed little effect on the velocity profiles. Tests with a hot wire anemometer failed to indicate any tendency to form Taylor vortices in the flow.

REFERENCES AND BIBLIOGRAPHY

1. STENNING, A.H., "The Turbulent Boundary Layer in Spiral Flow", S.M. Thesis, M.I.T. Department of Mechanical Engineering, July, 1951.

2. TAYLOR, E.S., "The Skewed Boundary Layer", A.S.M.E. Preprint 58-A-113, 1959.

3. JOHNSTON, J.P., "Three-Dimensional Turbulent Boundary Layer", M.I.T. Gas Turbine Laboratory Report No. 39, May, 1957.

4. "Turbomachinery Notes", M.I.T. Gas Turbine Laboratory, Unpublished Collection of Design Criteria.

5. LIMA, H., "Yaw Probes in a Total Pressure Gradient", S.M. Thesis, M.I.T. Department of Mechanical Engineering, January, 1958.

6. ISENBERG, J.S. and STENNING, A.H.,"Laminar And Turbulent Boundary Layer In A Rotating Pipe", M.I.T. Gas Turbine Laboratory, June, 1952.

7. SCHLICHTING, H., "Boundary Layer Theory", Pergamon Press, New York,1955.

Fig. 1.
WIND TUNNEL

Fig. 3.
TELEDELTOS PAPER - INTAKE NOZZLE PROFILE

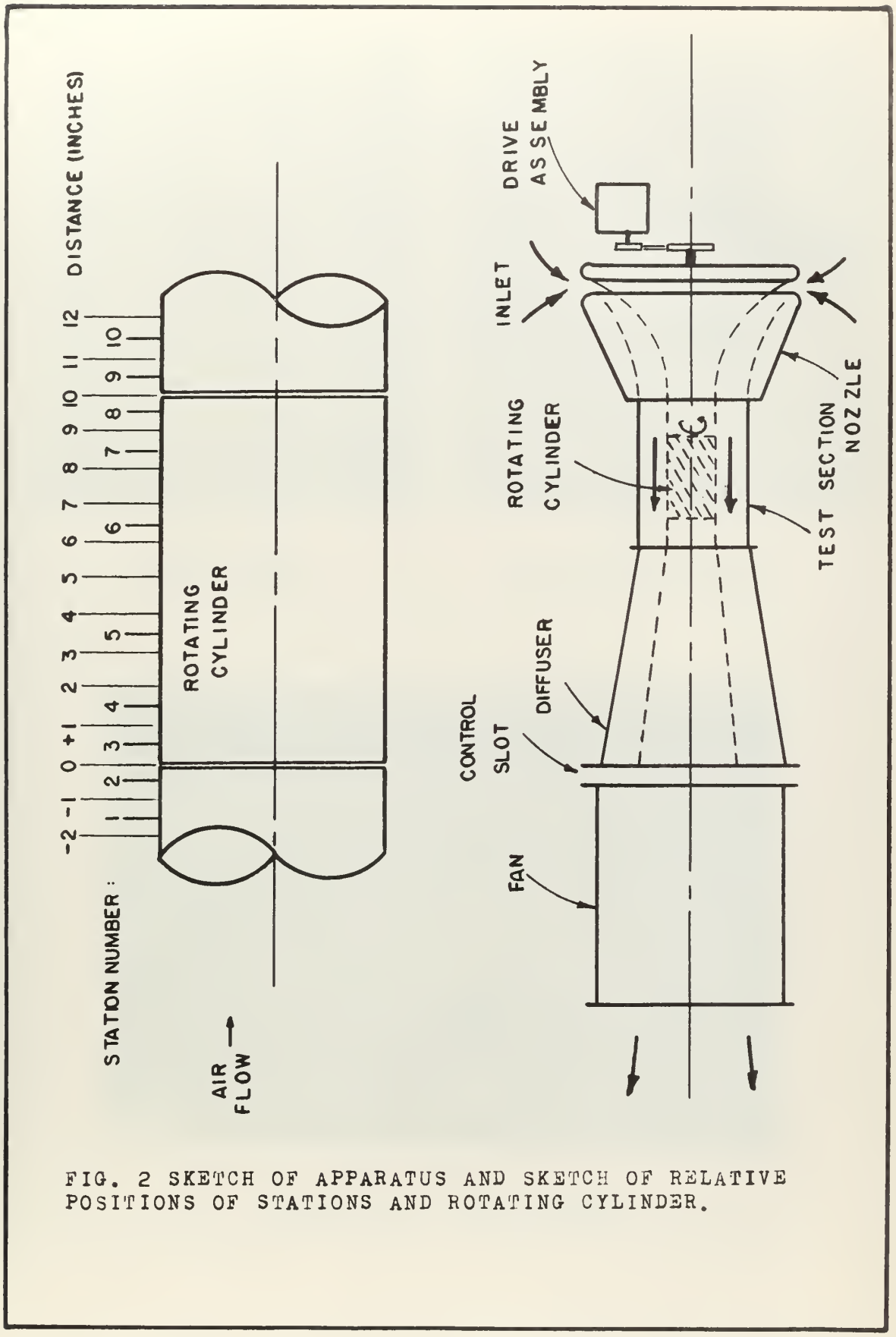

FIG. 2 SKETCH OF APPARATUS AND SKETCH OF RELATIVE POSITIONS OF STATIONS AND ROTATING CYLINDER.

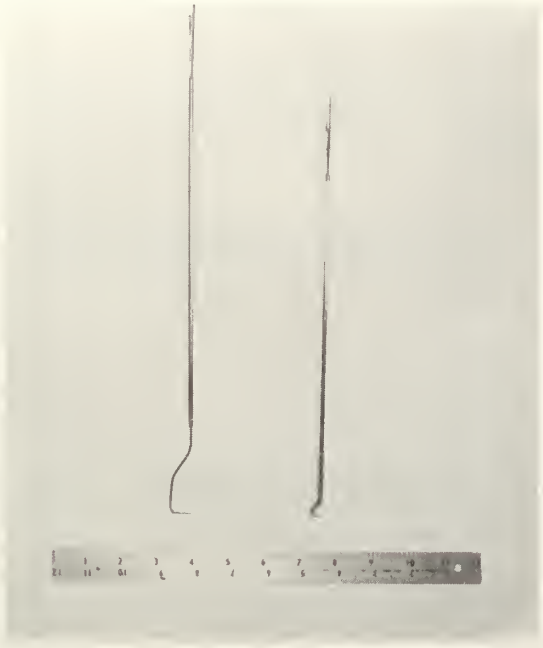

FIG. 4.
COBRA PROBES

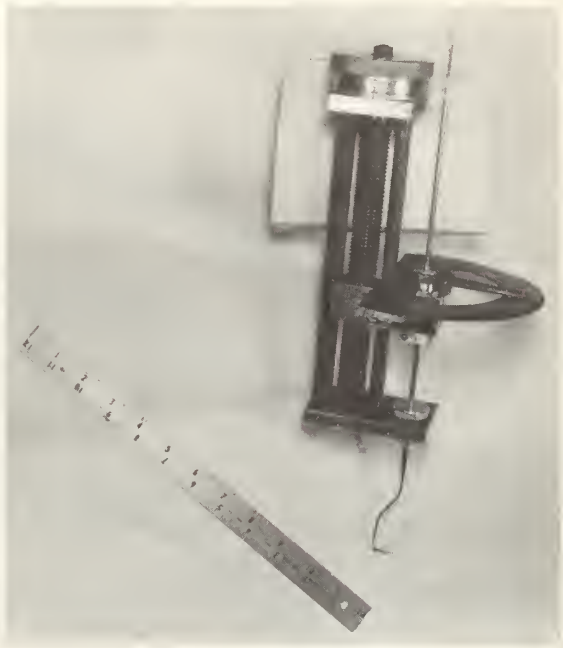

FIG. 5.
TRAVERSING DEVICE

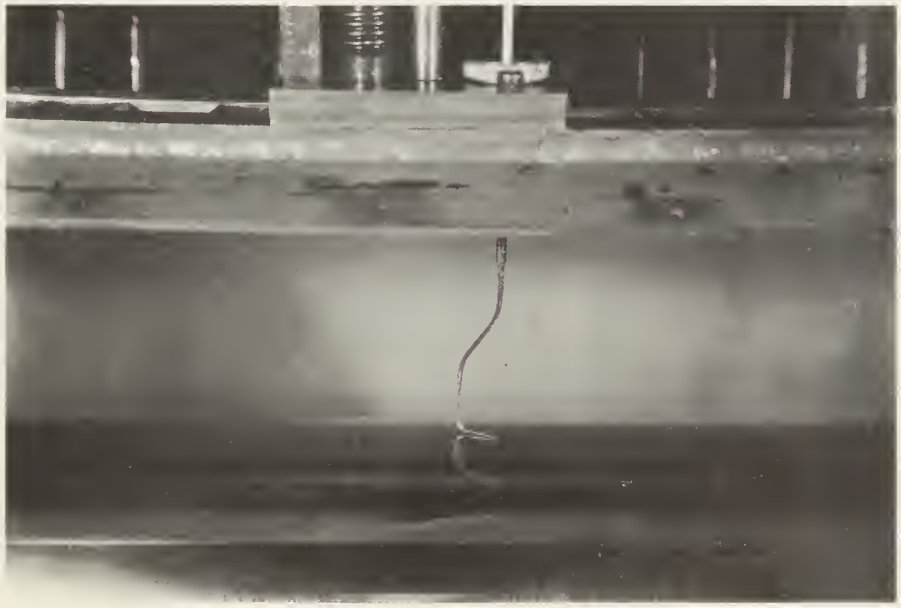

FIG. 6.
PROBE "B" IN TEST SECTION

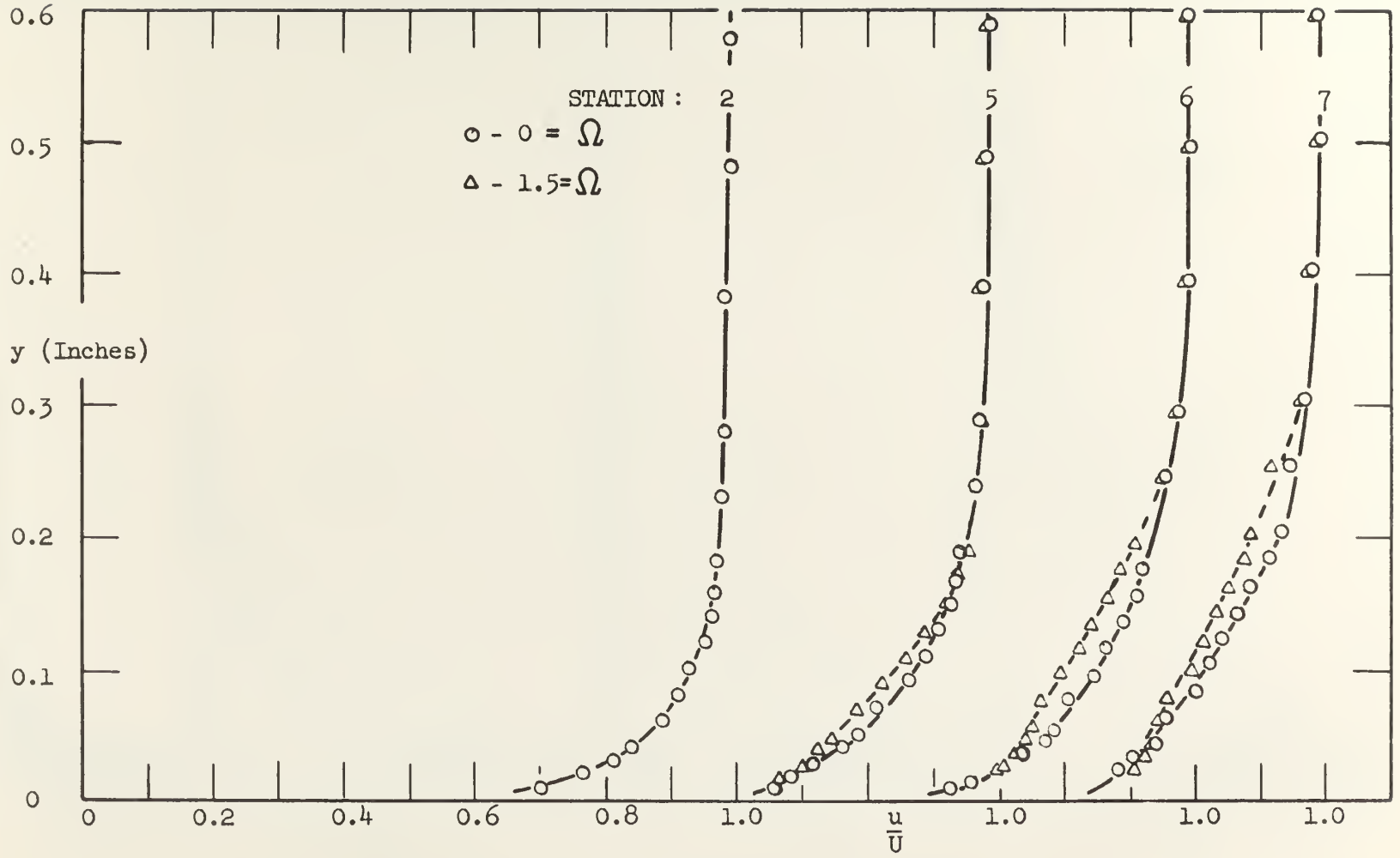

FIG. 7. AXIAL VELOCITY PROFILES AT ALL STATIONS (U = 67, Ω = 0,1.5)

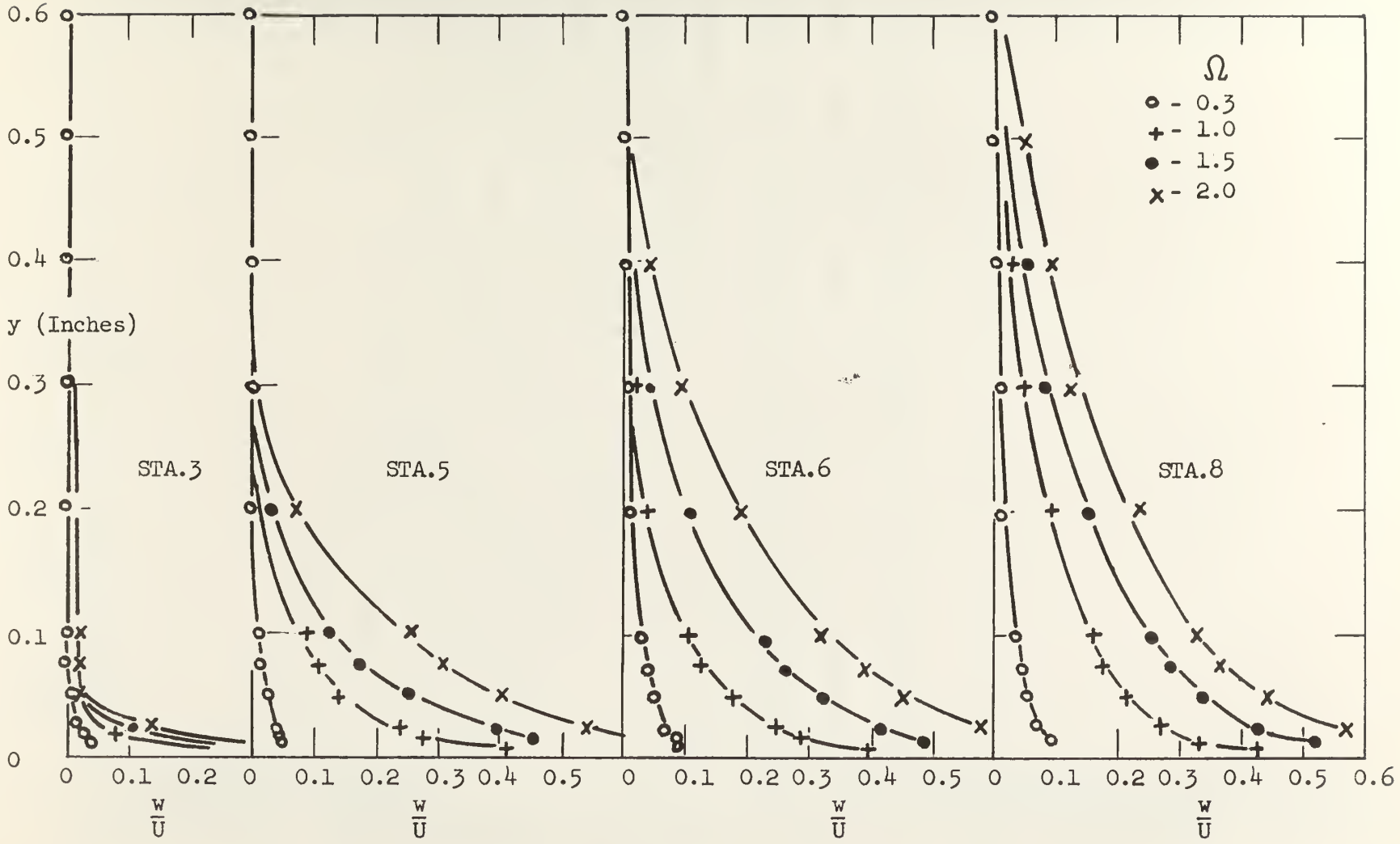

FIG. 8. TRANSVERSE VELOCITY PROFILES AT ALL STATIONS (U = 50)

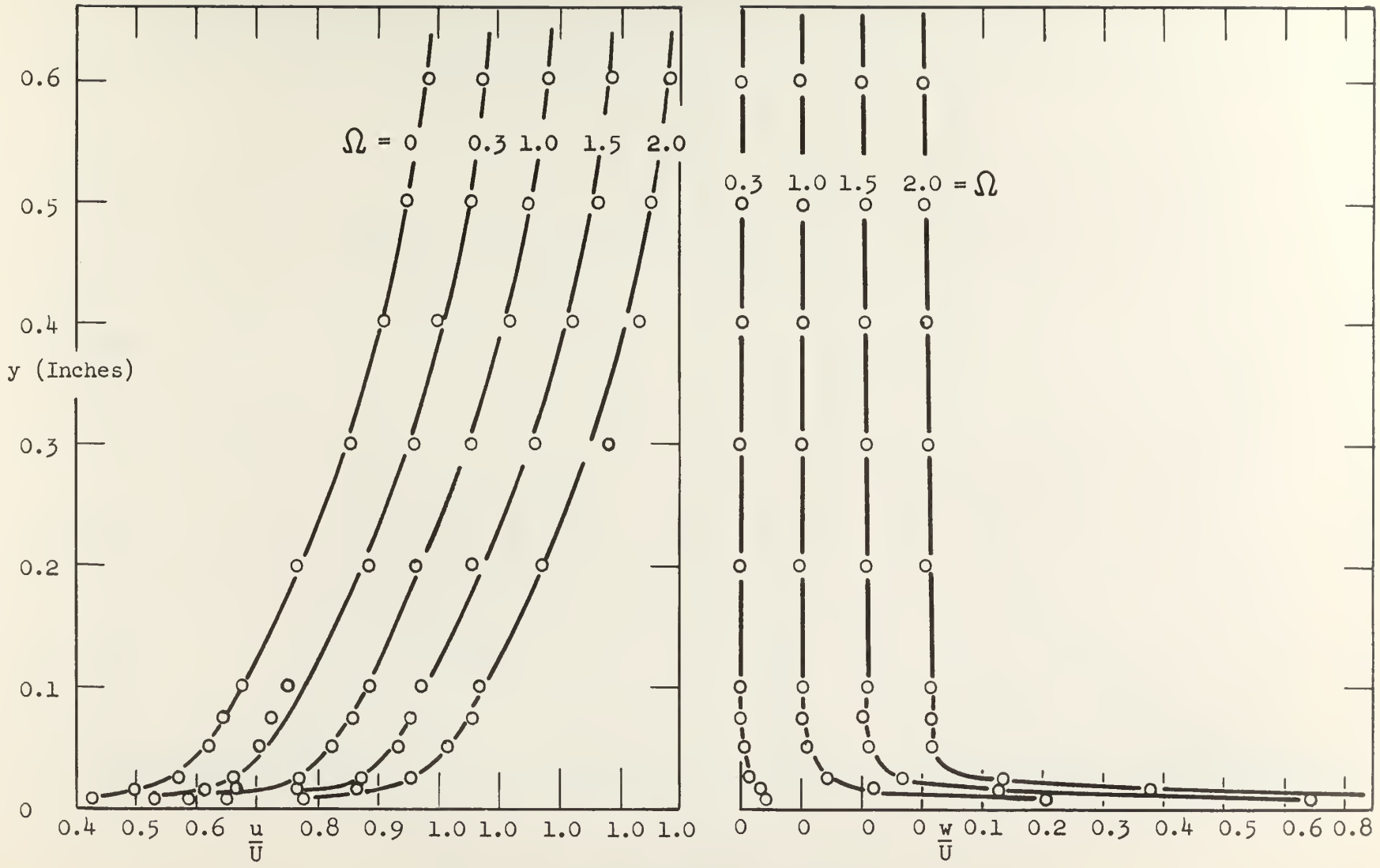

FIG. 9. VELOCITY PROFILES AT STATION 3 (U= 50)

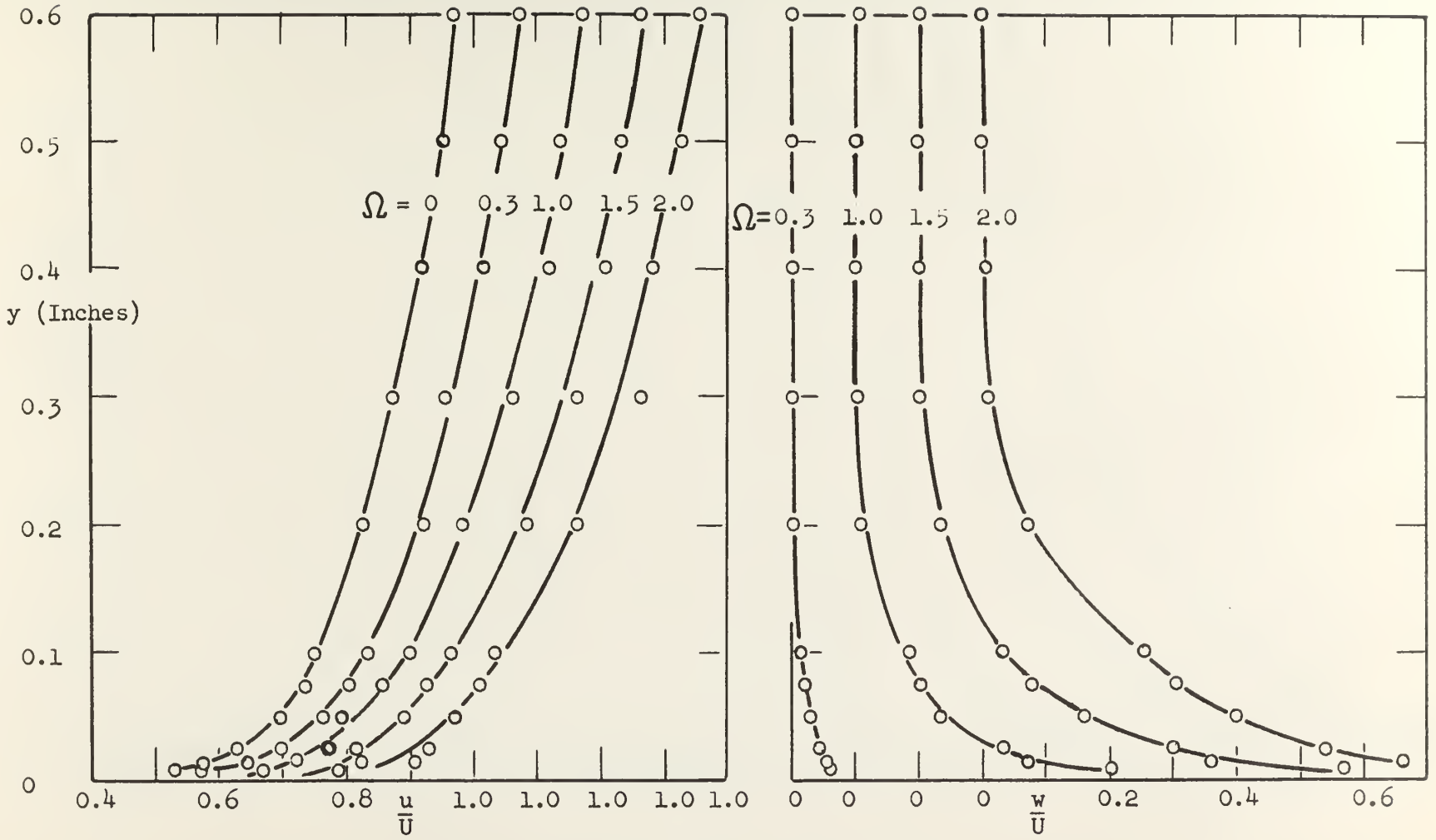

FIG.10. VELOCITY PROFILES AT STATION 5 (U = 50)

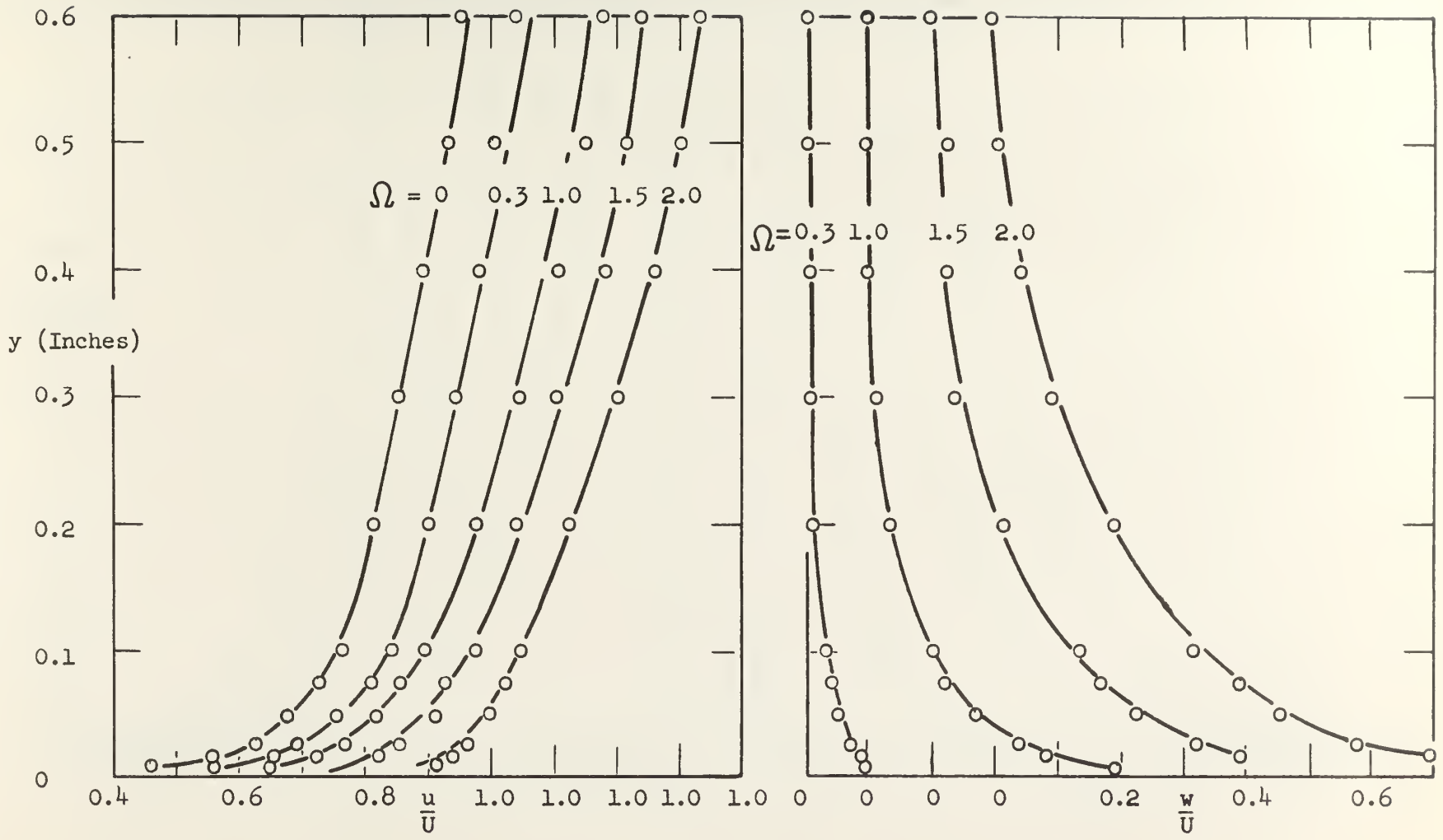

FIG.11. VELOCITY PROFILES AT STATION 6 (U = 50)

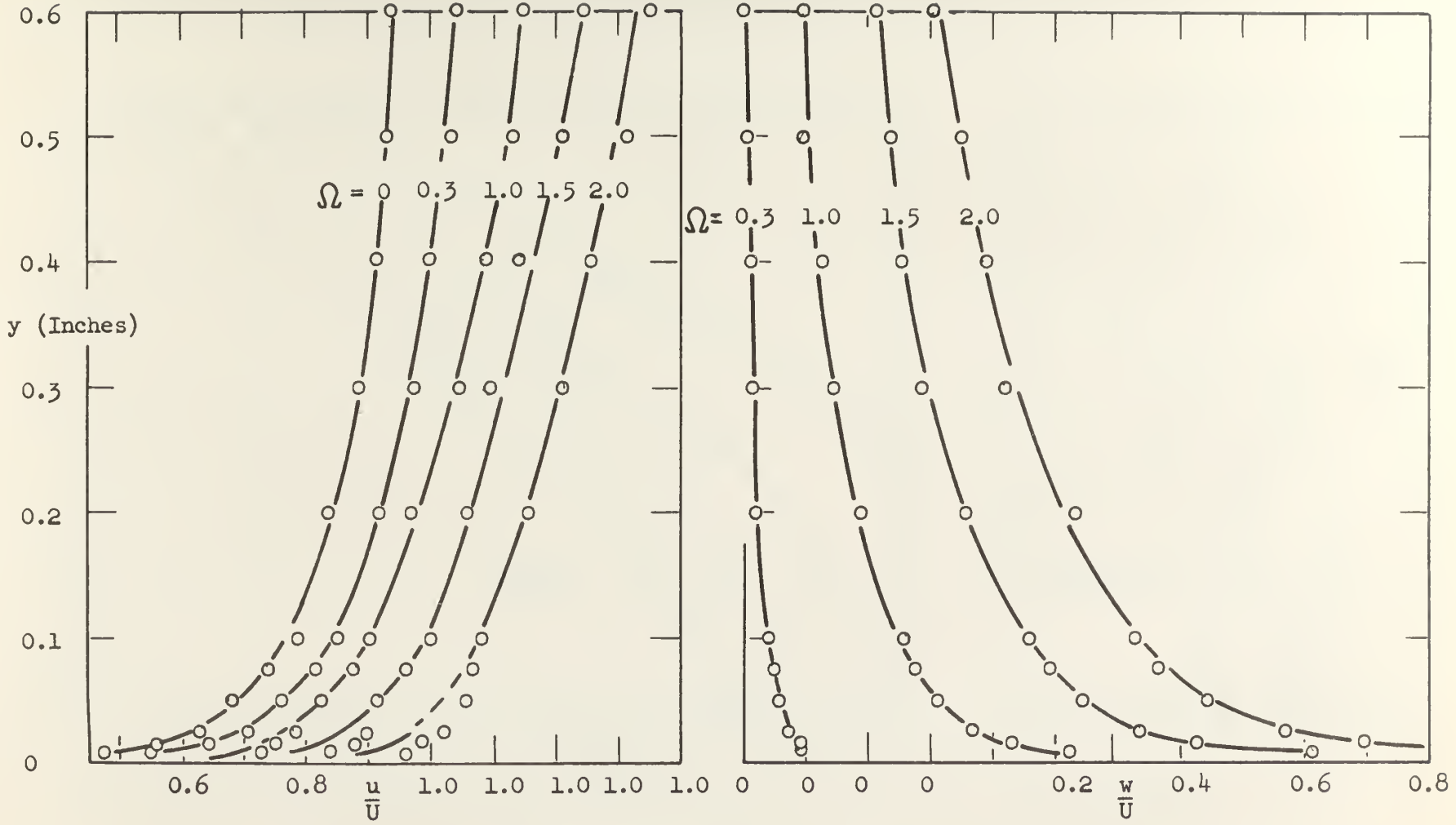

FIG. 12. VELOCITY PROFILES AT STATION 8 (U = 50)

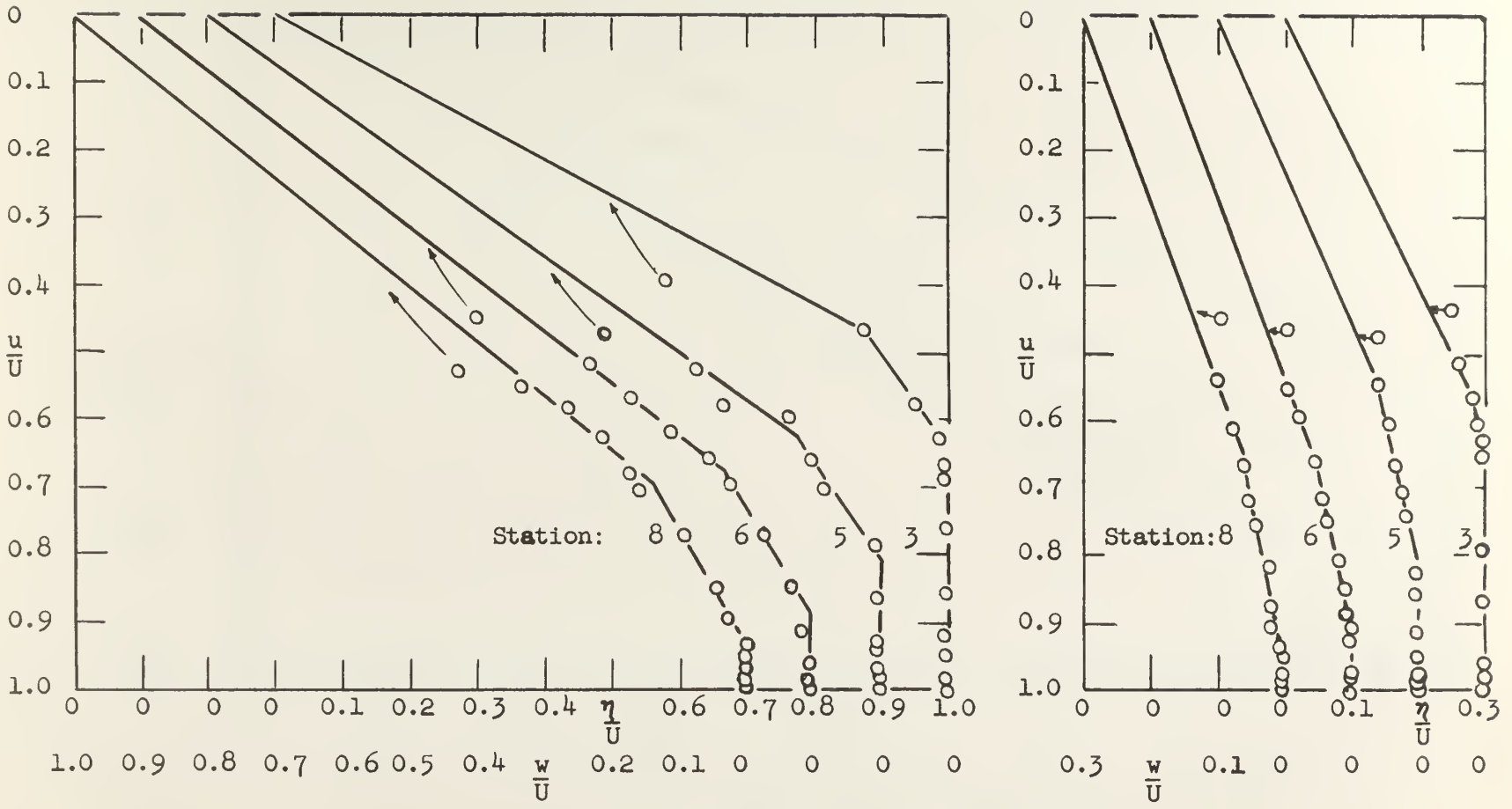

FIG. 13. POLAR PLOTS OF VELOCITY PROFILES (U = 50, Ω = 0.3,1.0)

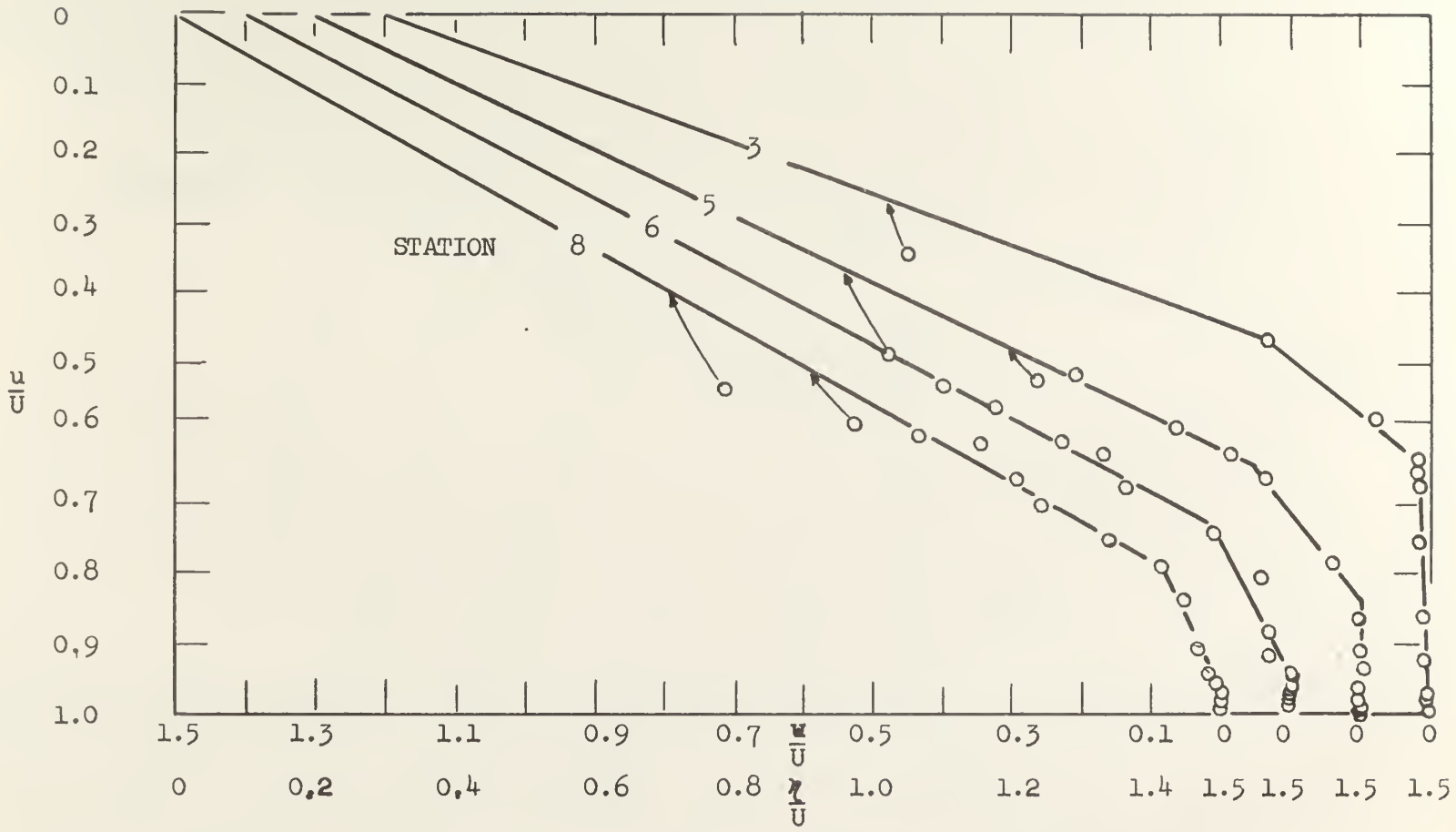

FIG. 14. POLAR PLOTS OF VELOCITY PROFILES (U= 50, Ω = 1.5)

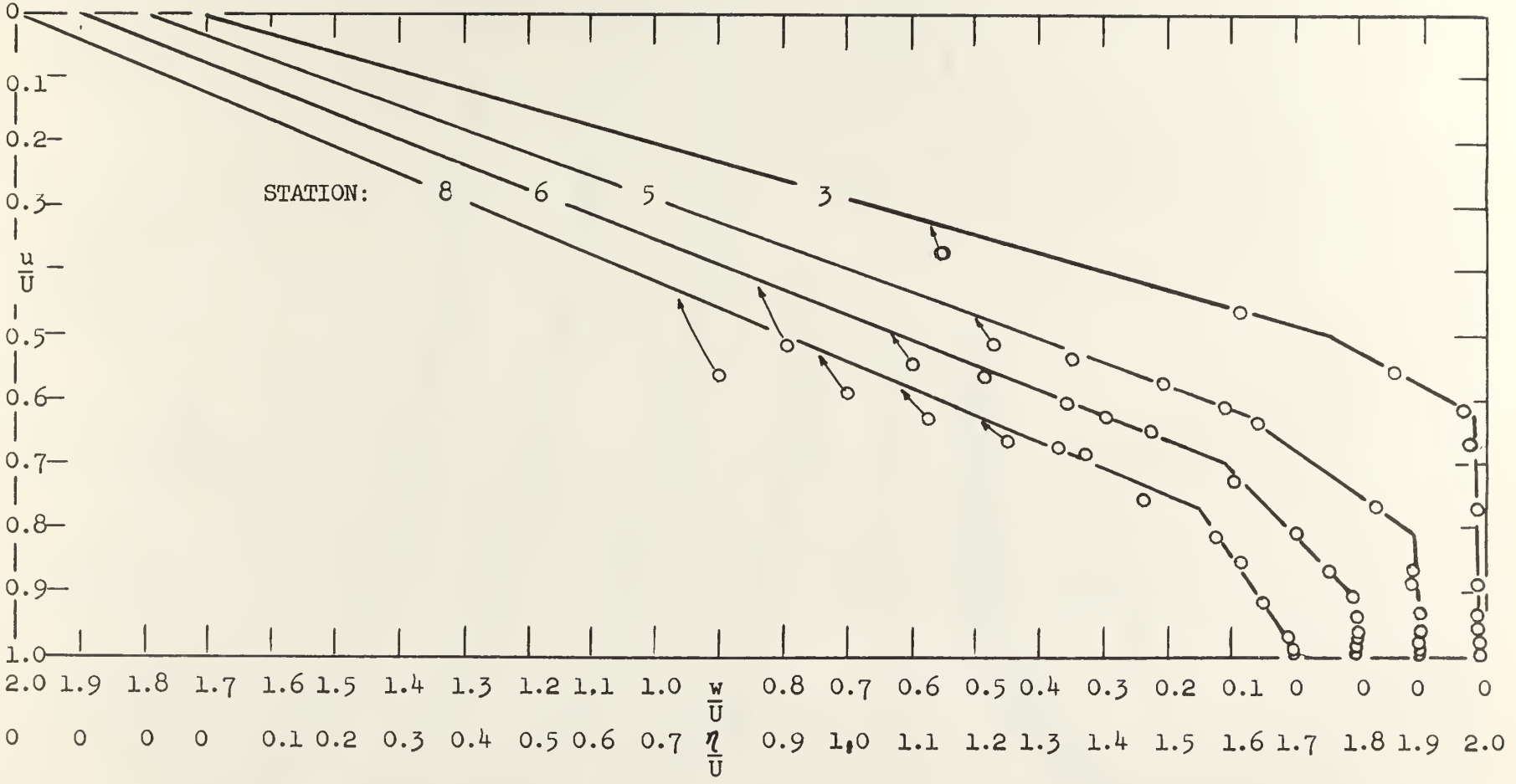

FIG. 15. POLAR PLOTS OF VELOCITY PROFILES (U = 50, Ω = 2.0)

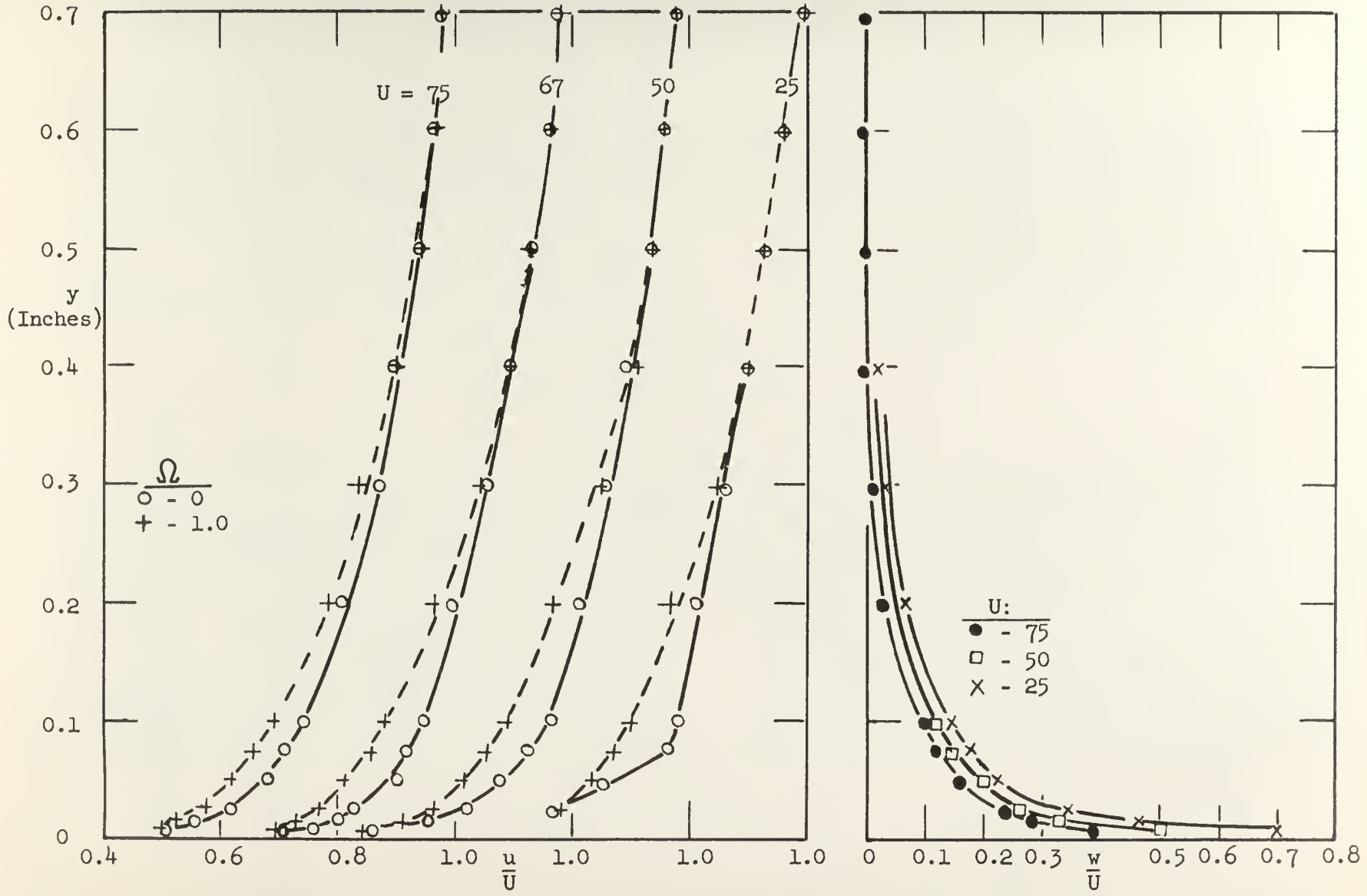

FIG. 16. EFFECT OF REYNOLDS NUMBER ON VELOCITY PROFILES (STATION 6)

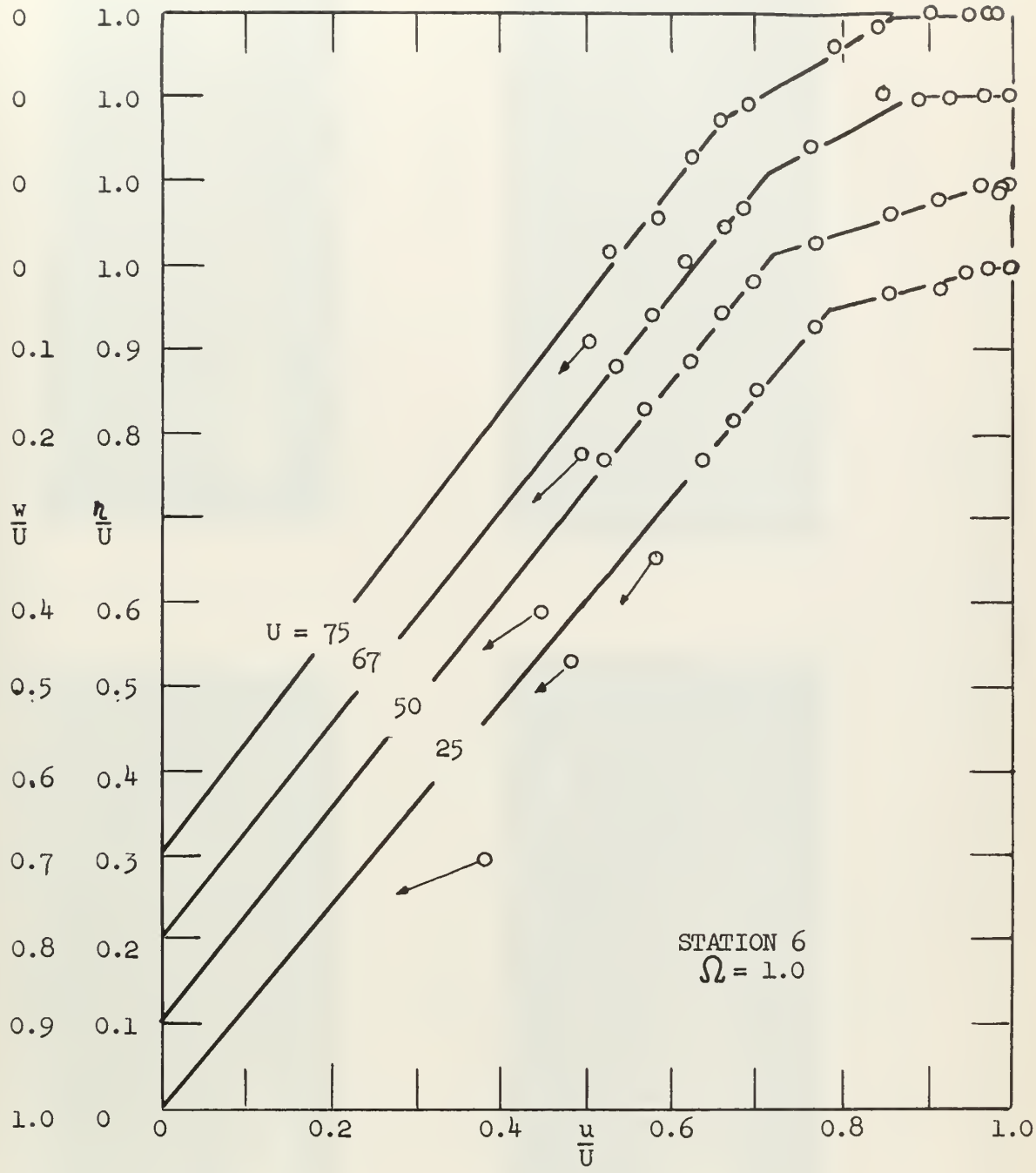

FIG. 17. POLAR PLOT OF REYNOLDS NUMBER EFFECT

Ω = 0.3

Ω = 1.0

Ω = 1.5

Ω = 2.0

FIG. 18. CARBON BLACK TRACES

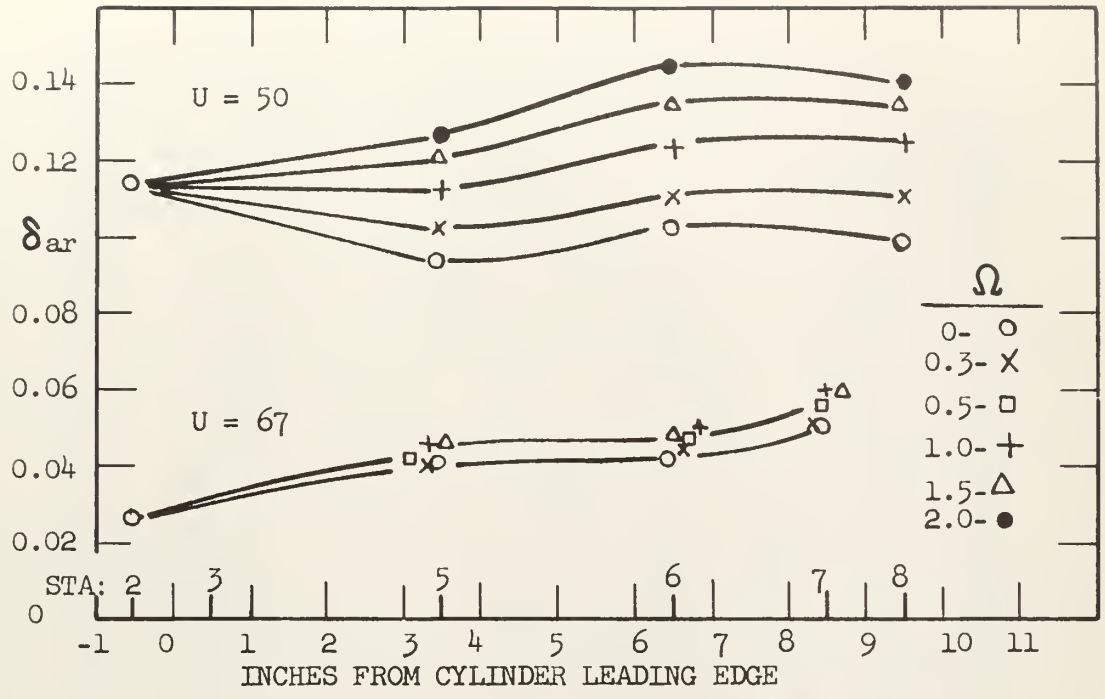

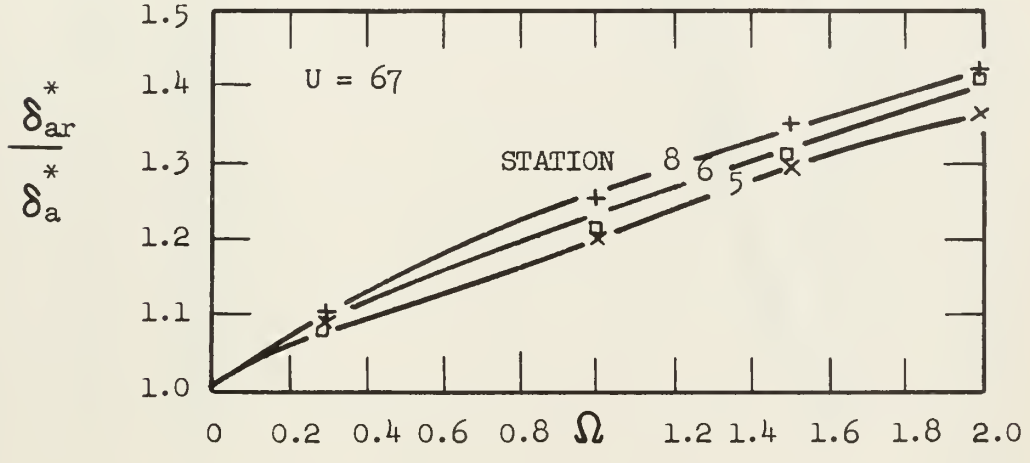

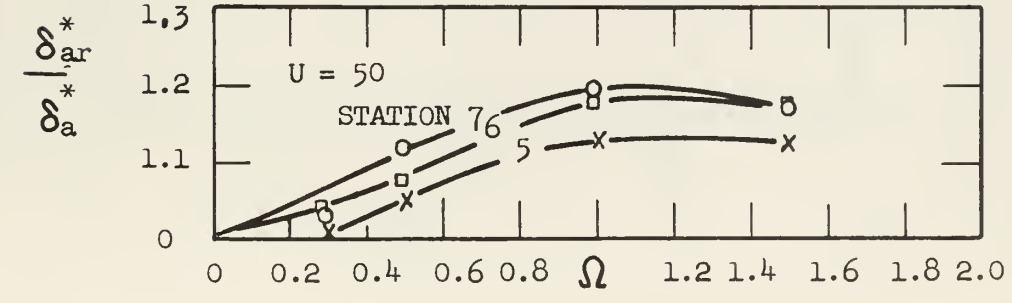

FIG. 19. DISPLACEMENT THICKNESS AND THICKENING FACTOR

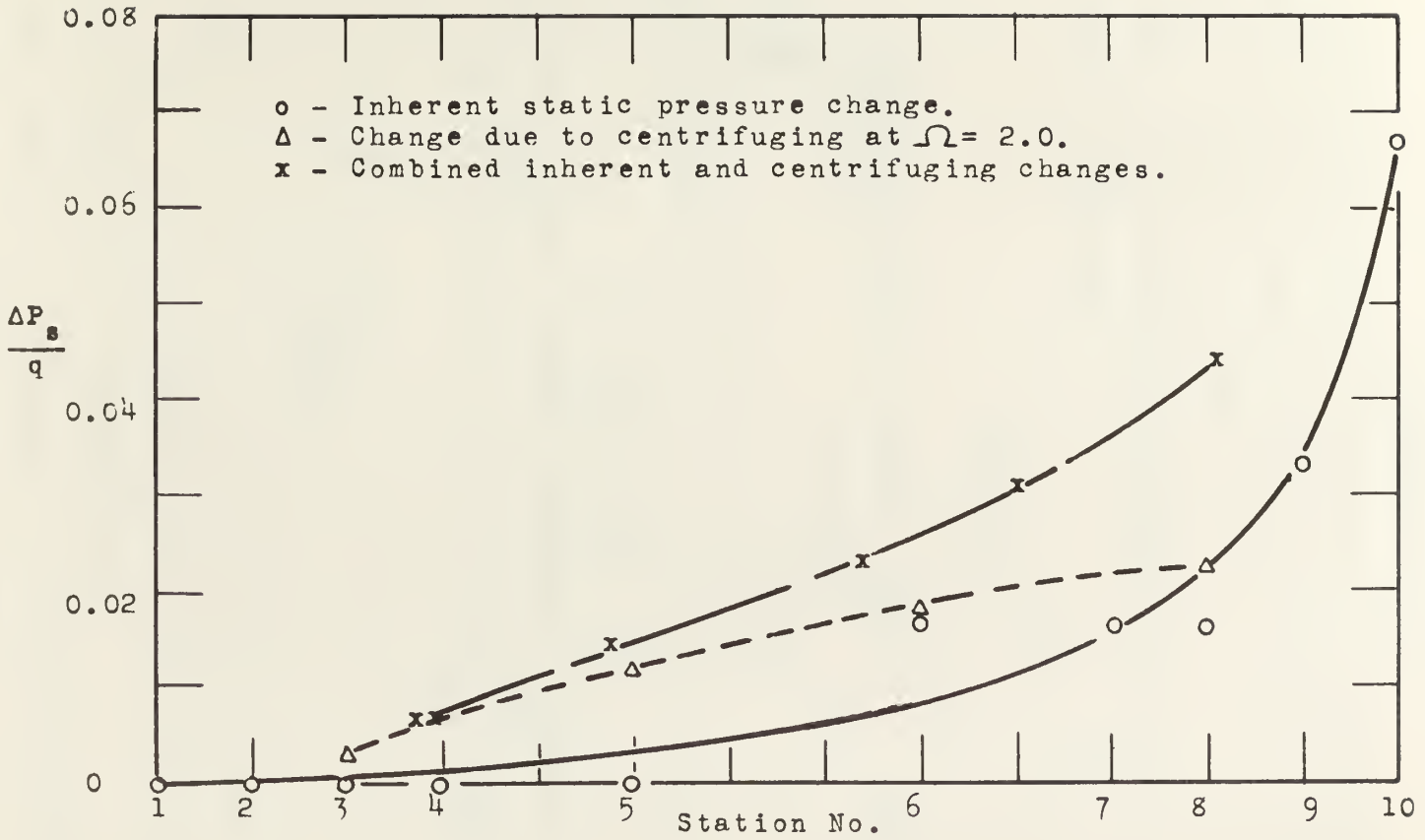

FIG. 20. STATIC PRESSURE CHANGE ALONG CYLINDER SURFACE (U = 50, Ω=2.0)

APPENDIX A

APPLICATION OF TELEDELTOS PAPER TO NOZZLE DESIGN

A method for applying the results of semi-conducting Teledeltos paper potential plotting technique to axially symmetric flow is described.

The flow is assumed irrotational and without a tangential velocity component.

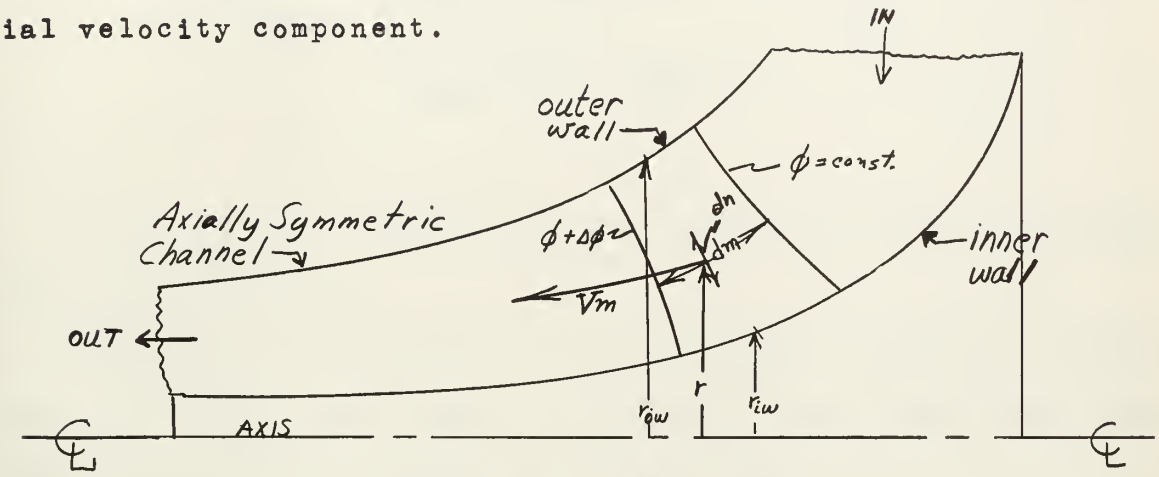

$$V_m = \frac{\partial \phi}{\partial m} = \frac{\Delta \phi}{\Delta m} = \frac{K}{\Delta m}$$

K can be determined from the continuity equation:

$$\dot{m} = \int_{r_{ow}}^{r_{iw}} (V_m \bar{\rho}\ 2\ \pi\ r)dn = 2\ \pi\ \bar{\rho} \int_{r_{ow}}^{r_{iw}} \left(\frac{K\ r}{dm}\right)dn$$

$$K = \frac{\dot{m}}{2\pi\rho} = \frac{1}{\int_{r_{ow}}^{r_{iw}} \left(\frac{r}{dm}\right)dn}$$

The value for r, Δm, and Δn can be found by direct measurement; $r\rho V_m$ plotted versus dn (ie., Δn), and a process of graphic integration will determine K.

The velocity at any point can be determined for each region bounded by equi-potential lines.

APPENDIX B

YAW MEASUREMENT ERROR

IN SKEWED FLOW

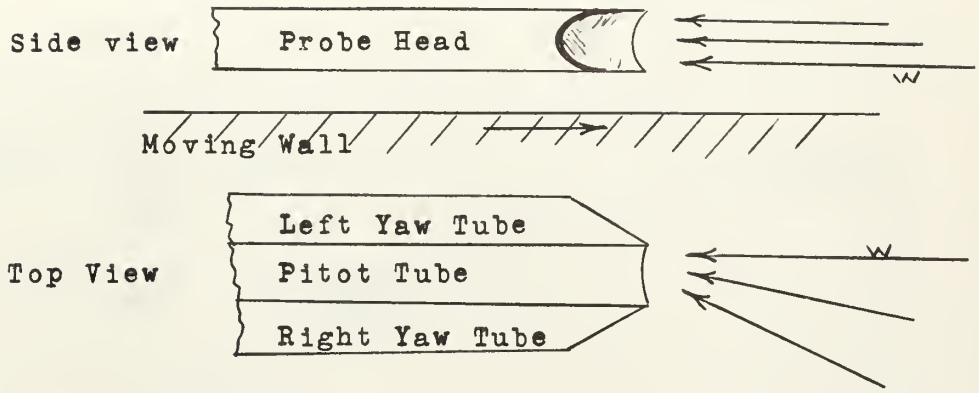

The yaw tubes read an average of the pressures over the area being sampled.

Assume the probe head is lowered into a skewed boundary layer such that the probe is directly in line with the stream-line closest to t he wall.

In this type of boundary being investigated, the trans-verse component has a larger gradient than the axial component in the region near the surface. Referring to the figure above, it can be seen that the left tube receives a larger pressure influence than the right tube since it is shielded from the skewed lower velocities by the geometry of the rest of the tube. The right tube reads the mean pressure which includes lower velocity stream-lines. Thus, the right reads a lower pressure than the left tube. To correct this unbalance, the operator moves the probe counter-clockwise and t he indication is a direction away from the transverse streamline.

APPENDIX C

VELOCITY VECTOR AND POLAR PLOT DESCRIPTION

The following figure depicts the various angles and velocity vectors. A typical data point "P" is shown and is representative of any point on the curve.

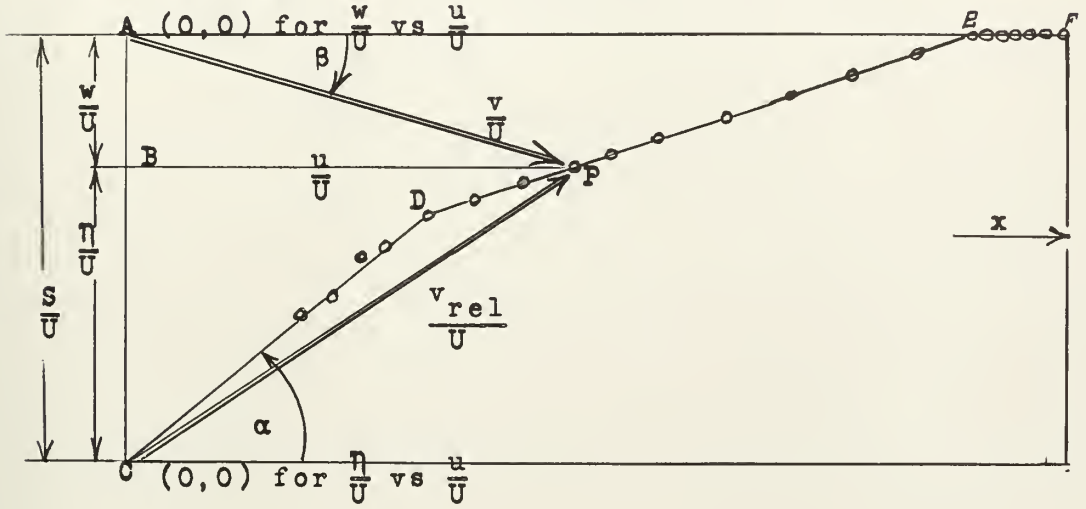

C-D-E-F: The curve of a typical polar plot.
C-D: Quasi-collateral portion of boundary layer that is collateral when viewed from the rotating cylinder.
D-E: Second quasi-collateral portion.
E-F: Remainder of boundary that is unaffected by rotation.
A-P: Velocity resultant vector as measured.
C-P: Velocity resultant vector as seen from rotating cylinder.
A-C: Surface velocity vector.
A-B: Transverse velocity component in fixed reference frame.
C-B: Transverse velocity component in rotating reference frame.
B-P: Axial velocity component common to both reference frames.
β : Angle of flow measured by yaw probe.
α : Angle of flow relative to cylinder; measured by carbon black traces.